# Accepted Manuscript

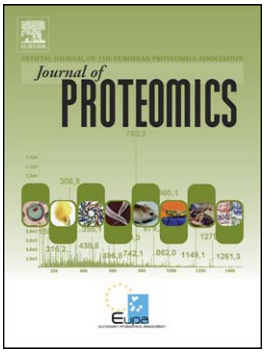


Global dynamics of *Escherichia coli* phosphoproteome in central carbon metabolism under changing culture conditions

SooA Lim, Esteban Marcellin, Shana Jacob, Lars K. Nielsen

PII: S1874-3919(15)30020-8
DOI: doi: 10.1016/j.jprot.2015.05.021
Reference: JPROT 2166

To appear in: *Journal of Proteomics*

Received date: 13 February 2015
Revised date: 13 May 2015
Accepted date: 20 May 2015

Please cite this article as: Lim SooA, Marcellin Esteban, Jacob Shana, Nielsen Lars K., Global dynamics of *Escherichia coli* phosphoproteome in central carbon metabolism under changing culture conditions, *Journal of Proteomics* (2015), doi: 10.1016/j.jprot.2015.05.021

# Global dynamics of *Escherichia coli* phosphoproteome in central carbon metabolism under changing culture conditions

SooA Lim[a], Esteban Marcellin[a*], Shana Jacob[a] and Lars K. Nielsen[a]

[a]Australian Institute for Bioengineering and Nanotechnology (AIBN), Corner College and Coopers Rd, The University of Queensland, St Lucia QLD 4072 Australia.

*Corresponding author at: Australian Institute for Bioengineering and Nanotechnology (AIBN), Corner College and Coopers Rd, The University of Queensland, St Lucia QLD 4072 Australia.

Tel.: + 61 7 334 63491; fax: + 61 7 334 63973; E-mail address: e.marcellin@uq.edu.au

Keywords: phosphoproteomics, quantitative phosphoproteomics, phosphorylation, central carbon metabolism

**Abstract**

Little is known about the role of global phosphorylation events in the control of prokaryote metabolism. By performing a detailed analysis of all protein phosphorylation events previously reported in *Escherichia coli*, dynamic changes in protein phosphorylation were elucidated under three different culture conditions. Using scheduled reaction monitoring, the phosphorylation ratios of 82 peptides corresponding to 71 proteins were quantified to establish whether serine (S), threonine (T) and tyrosine (Y) phosphorylation events displayed a dynamic profile under changing culture conditions. The ratio of phosphorylation for 23 enzymes from central carbon metabolism was found to be dynamic. The data presented contributes to our understanding of the global role of phosphorylation in bacterial metabolism and highlight that phosphorylation is an important, yet poorly understood, regulatory mechanism of metabolism control in bacteria.

Biological significance

The findings in this manuscript provide novel scientific knowledge about protein phosphorylation in dynamic regulation of the central carbon metabolism of *E. coli*. Evidence has accumulated confirming that phosphorylation is prevalently present in bacteria and has important regulatory roles of control of the central carbon metabolism. This investigation goes beyond data collections and shows that protein phosphorylation is quantitatively significant and varies under changing culture conditions.

## 1. Introduction

Bacterial cells adapt to rapid and drastic environmental changes by turning ‘on’ and ‘off’ specific subsets of proteins. Post-translational modifications are the fastest regulatory mechanism by which microorganisms regulate protein activity[1]. Protein phosphorylation, widely distributed in all living organisms, is the most prominent and most studied protein modification. Phosphorylation controls biological functions by inducing conformational changes in the protein’s active site or by regulating protein interactions with other proteins [2-7].

In prokaryotes, protein phosphorylation of histidine (H) and aspartate (D) residues occurs commonly as part of two component signalling systems and has been extensively studied [8]. Two component systems rely on high fidelity of recognition between the kinase and the response regulator. Several auxiliary regulators, which interfere with these highly specific phosphotransfer reactions have been reported in the last decade[9]. They act either on the sensory kinases or the response regulators to accomplish signal integration. Accompanying these regulators, increasing evidence shows that phosphorylation of serine (S), threonine (T) and tyrosine (Y) in bacteria, also regulates numerous physiological processes in bacteria, including key aspects of the central carbon metabolism [10-13].

Mass spectrometry based phosphoproteomic studies in *Escherichia coli* (*E. coli*), *Bacillus subtilis* (*B. subtilis)* and *Lactococcus lactis (L. lactis)* [14-16] confirmed earlier evidence from gel based proteomics [17, 18] that S/T/Y phosphorylation is far more widespread in bacteria than suggested by the few well-known examples, e.g., HPr kinase/phosphorylases [19-22] and

isocitrate dehydrogenase (Icd) [23-25]. Since then, investigations have flourished; reports have emerged of S/T/Y phosphorylation in *Klebsiella pneumoniae* [26], *Pseudomonas spp.*[27], *Streptomyces coelicolor* [28, 29], *Streptococcus pneumoniae* [30], *Mycoplasma pneumoniae* [31], *Listeria monocytogenes* [32], *Helicobacter pylori* [33], *Clostridium acetobutylicum* [34], *Rhodopseudomonas palustris* [35], *Thermus thermophiles* [36], *Synechococcus sp* [37], *Staphylococcus aureus* [38], *Acinetobacter baumannii* [39], *Saccharopolyspora erythraea* [40], and *Mycobacterium tuberculosis* [41] amongst others. Conservation across species of phosphorylation sites in enzymes from the central carbon metabolism in pathways for glycolysis, pentose phosphate and the tricarboxylic acid (TCA) cycle, suggests that phosphorylation plays a pivotal role in regulating central carbon metabolism. Previous studies have also linked S/T/Y phosphorylation to regulation of cell differentiation [29], physiology [42, 43], stress [44, 45], virulence and pathogenicity [46-50].

The majority of bacterial phosphoproteomic studies have focused on phosphor site discovery. However, there is a significant step from the discovery of a phosphor site to assigning biological function and identifying the control mechanisms and relevant phosphokinase and phosphatase. It is often difficult to correctly assign the phosphor site and even when assignment is possible, many discovered sites are likely to be spurious signals due to non-specific kinase activity and phosphor-transfer during mass spectrometry [51]. For example, of the 105 phosphor sites originally reported by Macek and colleagues for *E. coli* growing in Luria-Bertani (LB) [15], only nine were found in their subsequent SILAC-based temporal study in glucose minimal M9 medium, while 141 new phosphor sites were reported [12]. It is unclear how many of these differences can be attributed to physiological responses (e.g., the absence of the well

characterized Icd phosphorylation in presence of glucose) as opposed to spurious signals in either dataset.

For phosphorylation to play a physiological relevant role in metabolic control, however, it must be quantitatively significant and vary under changing culture conditions. In this study, we undertook a detailed quantitative evaluation of all phosphorylation events reported in the first *E. coli* phosphoproteome study grown on three carbon sources. Using scheduled reaction monitoring, we characterised the phosphorylation profile of 82 peptides, of which 71 proteins were differentially phosphorylated, and found that 23 enzymes from the central carbon metabolism displayed a distinct pattern of phosphorylation. These results confirm the process of phosphorylation as a key, yet poorly understood, regulator of *E. coli* metabolism.

## 2. Material and methods

### 2.1 *Strain & Culture Conditions*

*E. coli* K-12 MG1655 (CGSC 7740) were initially grown on LB medium. Seed cultures were washed three times with fresh minimal medium (R/2 (supplemented with 20g/L of glucose) (51) or M9 (supplemented with 2g/L acetate) (50)) and transferred to shake flasks (2L cultured at a working volume of 400mL) cultured in a shaking incubator set to 37℃. Then, cells were cultured on each medium (LB, glucose, acetate) using a bioreactor (DasGip Control 4.0, Germany). Bioreactor cultures were performed at a working volume of 400 mL, at constant pH 6.8 and a constant airflow of 0.375 v.v.m. Dissolved oxygen tension was controlled above 30% by agitation first and then by mixing air with pure oxygen. Cell growth was monitored by measuring the absorbance at 600nm (Libra S4, Biochrom Ltd, United Kingdom [UK]).

### 2.2 *Protein extractions*

Cells harvested in mid-exponential phase were centrifuged at 5,250 rpm (Allegra X15R, Beckman Coulter, United States [US]) for 10 minutes at 4°C, washed once (washing buffer: 100mM NaCl, 25mM Tris-HCl, pH7.5) and resuspended in lysis buffer as described elsewhere with minor modifications [14]. Homogenous cell disruption was achieved by mechanical disruption using 0.1 mm glass beads (5 × 1 min, 4800 rpm). Cellular debris was removed by centrifugation (13,000 rpm for 10min at 4ºC, microfuge 22R, Beckman coulter, US) and the lysate treated with DNase I (Fermentas) and RNase A (Fermentas). The crude protein extract was extensively dialyzed against MilliQ water containing protease inhibitors using Slide-A-Lyzer cassettes (3500MWCO, Thermo Scientific, US) and protein content was quantified using

2D Quant kit (GE Healthcare, US). Finally, protein extracts were concentrated by lyophilization and stored at -20°C until protein digestion.

2.3 *Protein Digestion*

Ten milligrams of lyophilized protein were dissolved in denaturing solution as described in [15] supplemented with 2% CHAPS to increase protein solubilization. Samples were reduced with DTT and alkylated with iodoacetamide as described previously [15]. Samples were diluted with 5 volumes of 10mM ammonium bicarbonate to reduce urea concentration, before being digested with LysC (lysyl endopeptidase) for three hours. Proteins were further digested overnight with trypsin (Promega Gold, MS grade) at 37ºC with gentle rocking. Prior to down-stream analysis, samples were concentrated by vacuum centrifugation (Eppendorf, Germany) and acidified to pH < 2.7 with 0.1% formic acid. Insoluble materials were removed by centrifugation and the samples dried using a vacuum centrifuge.

2.4 *Estimation of the lower limit of detection (LLD) for α-casein*

To estimate the LLD for *α-casein*, commercial phosphorylated and unphosphorylated *α-casein* (Sigma Aldrich, C8032, C6780) were used. *α-casein* was digested with trypsin (Promega, sequencing grade) overnight. Subsequently, *α-casein* on its phosphorylated and unphosphorylated form was mixed in cellular lysates or distilled water at various concentrations to determine the lower level of detection of mass spectrometer (Nano-LC QSTAR Elite). To assess the sensitive of sMRM, samples supplemented with different amounts of unphosphorylated α-casein and a constant amount of phosphorylated *α-casein* were injected in an LC coupled to a QTRAP (Applied Biosystems, US).

2.5 *Phosphopeptide Enrichment*

Strong Cation Exchange (SCX) was performed as described elsewhere [14]. Briefly, samples were loaded onto a Resource S column (GE Healthcare, US) in 100% solvent A (5mM $KH_2PO_4$, 30% acetonitrile, 0.1% trifluoroacetic acid, pH = 2.7) at a flow rate of 1 ml/min. Elution was performed with a gradient of 0 – 30% solvent B (5mM $KH_2PO_4$, 30% acetonitrile, 350mM KCl, 0.1% trifluoroacetic acid, pH2.7) over 30 min. Seventeen 2-ml fractions were collected, desalted (Sep-Pak tC18, Waters) and concentrated by vacuum centrifugation [52]. The dried samples were acidified with 0.1% formic acid and enriched using Phos-$TiO_2$ kit (GL Sciences Inc., US) according to the manufacturer's protocol.

2.6 *Protein identification*

Protein discovery was performed using a in a Nano-LC QSTAR Elite (AB Sciex, US). Peptides were separated on a $C_{18}$ column (Vydac MS C18 300 Å 150mm × 0.3mm, GRACE Davison, Discovery Sciences, USA) operated at 30°C with a gradient running from 0 to 80% acetonitrile (in 0.1% formic acid) for 105 minutes at a flow rate of 3 µl/min. Proteins were identified by information-dependent acquisition of the fragmentation spectra of charged peptides with a precursor selection window of 100 to 1800 m/z using enhanced pulsed extraction of fragments. Tandem mass spectra were acquired for 1 s and fragmented peptides were selected for sequencing for 12 s in positive mode. Data were acquired using Analyst software and peptides were identified using the paragon algorithm (Protein Pilot software 4.0, Applied Biosystems, US) [53] and Mascot. All searches were conducted as described by Macek et al [15], using thorough search, FDR, two missed-cleavages, trypsin, iodoacetamyde and DTT and manual inspection for "good" b and y ions.

2.7 *Quantitative analysis*

Scheduled multiple reaction monitoring (sMRM) was used to quantify phosphorylated peptides using either a QTRAP 5500 or a QTRAP 4000 (Applied Biosystems, US) depending on instrument availability [54, 55]. Peptides were separated on an analytical column (100mm × 2.1mm 2.6µm 100Å Kinetix $C_{18}$, Phenomenex, US) using a 2 to 80% acetonitrile (in MilliQ water with 0.1% formic acid) gradient over 100 minutes. Eluted peptides were analyzed in positive ion mode. All sMRM coordinates were developed and optimized using MRMPilot (Applied Biosystems, US) as described by the software manufacturer.

2.8 *Statistical analysis*

Initial quantitation was performed in Analyst (1.5.2, Applied Biosystems, US) or MSQuant. Each peak was manually inspected and peptides with unfavourable elution profile (bad resolution), interfering noise or inconsistent elution time across biological and technical repeats were excluded from the analysis. Peak areas were normalized between samples using spiked in α-casein as an external standard and log transformed to satisfy the linear model assumption of residual normality and variance homogeneity. After normalization, data was analyzed using linear models in R.

2.9 *Targeted open scan and validation of phosphorylation sites*

In order to validate the phosphorylation site of the previously reported S/T/Y phosphorylation site, all the precursor masses previously reported to be phosphorylated were subjected to MS/MS in the Nano-LC hybrid Triple-TOF 5600 (AB Sciex, US). The LC conditions were reduced to 60 minutes and the search parameters were the same as the reported above. The raw MS/MS spectra

were submitted for search using Protein Pilot against the *E. coli* genome and a decoy database of common contaminants and manually inspected using Peak View. Finally, sMRM were designed for the unique phosphorylation ions on the QTRAP.

## 3. Results

### 3.1 *Identification of phosphopeptides in discovery mode*

The original paper by Macek *et al.* (2008) [15] used phosphopeptide enrichment and high resolution Orbitrap analysis to identify 105 phosphopeptides when cells grew on LB. In order to gain a sense of the abundance of phosphopeptides, we performed an information-dependent acquisition (IDA) mode experiment using a Nano-LC QSTAR Elite on samples from both acetate and glucose based minimal media. This also provided an opportunity to explore if new phosphorylation events could be detected.

Total protein lysates were fractionated by SCX and analyzed in IDA scan mode. More than 2,400 high-confidence peptides were identified in both glucose and acetate, corresponding to 559 and 526 unique proteins, respectively (at least 2 peptides with greater than 99% confidence) (Supplementary Table S1a). A total of 52 out of the 79 proteins previously reported to be phosphorylated were found, including 37 of the 105 reported peptides in their unphosphorylated form. After $TiO_2$ enrichment however, only 11 of the 105 original phosphopeptides were detected in either glucose or acetate samples (Supplementary Table S1b and Fig. S1). Another 23 high-confidence phosphopeptides were discovered, but surprisingly none of these were among the 141 new phosphor sites reported in the second *E. coli* paper [12] despite this study also using glucose minimal M9 medium.

Unsurprisingly, the phosphopeptides overall discovery rate was lower on a Nano-LC QSTAR Elite than an Orbitrap. Orbitrap instruments are able to use higher-energy collisional dissociation (HCD) and electron transfer dissociation (ETD) for fragmentation while the QSATR can only do collision induced dissociation (CID). However, considering the modest discovery rate for the unphosphorylated cognates, the data does not support the notion of phosphopeptides being inherently more difficult to detect by ESI-MS/MS [51] than by Orbitrap. This is further supported by the fact that the lower limit of detection (LLD) is similar for α-casein phosphopeptides and their unphosphorylated cognates (Fig. 1A). The LLD for unphosphorylated peptides was slightly lower in distilled water, but similar went spiked into a complex matrix of *E. coli* protein digest.

It is clear that our poor discovery rate of phosphopeptides can largely be attributed to the use of a QSTAR rather than a next generation LC for protein discovery; however these findings highlight a possible lack of careful evaluation of phosphorylation sites reported in the literature.

### 3.2 *Validation of sMRM approach to quantify ratios of phosphorylation*

In order to quantify both the extent of phosphorylation and any changes in response to medium changes, we developed targeted analysis using sMRM, the most sensitive MS technique for quantitative proteomics [54-57]. We first validated the technique using an sMRM protocol optimised for phosphorylated and unphosphorylated peptides of α-casein (Fig. 1B–C). The sMRM response was linear (Fig. 1B) and highly reproducible (Fig. 1C). The response vary for individual transitions; in some instances the best phosphopeptides transition has a stronger signal than the best unphosphorylated cognate transition, in other instances the opposite is true. Overall,

we did not observe the general suppression of the phosphopeptide signal reported previously for ESI [51] .

< FIG. 1>

3.3 *Phosphorylation ratios changed under changing culture conditions*

sMRM proved reliable for detecting phosphopeptides at very low LLD, even in complex samples. Therefore, we designed sMRM transitions for at least two detected secondary ions for each of the 105 phosphorylated peptides reported previously [15] as well as their unphosphorylated cognates. The designed sMRM transitions were evaluated for cultures on acetate, glucose and LB medium and the best transition for each peptide chosen for subsequent analysis (Supplementary Table S2a). In contrast to the low discovery rate using IDA in this study and in the recent *E. coli* publication [12], sMRM detection was achieved for 82 phosphopeptides and 87 unphosphorylated cognates in unenriched samples (Supplementary Table S2b). This result confirms that sMRM is a reliable technique for quantitative analysis of the *E. coli* phosphoproteome.

Replicate cultures on acetate, glucose and LB medium were analyzed using sMRM and the results normalised against an internal standard (α-casein). The phosphorylation ratio varied significantly for 58 of all detected peptides, including 19 of 23 peptides from central carbon metabolism enzymes (Fig. 2, Supplementary Table S2c-d). This supports the idea that protein phosphorylation plays a crucial role in regulatory processes such as cell cycle control, receptor-mediated signal transduction, differentiation, proliferation, transformation, and metabolism [58-

60].Given the prevalence of central carbon metabolism enzymes, we restricted our analysis to this subset of enzymes.

< FIG. 2>

Changes in phosphorylation ratios were observed for four enzymes in the TCA cycle, including Icd. Given the amount of information in the literature regarding this enzyme, we used this phosphorylation to assess the quality of our approach. As expected, Icd phosphorylation increased dramatically when grown on acetate (Fig. 3A–C); the phosphorylation ratio was 7.22 times higher ($p < 10^{-6}$) than when cells where grown on glucose. Other enzymes from the TCA cycle all had lower ratios of phosphorylation: 1.3-fold ($p = 0.0074$) for malate dehydrogenase (Mdh), 4.5-fold ($p < 10^{-6}$) for phosphoenolpyruvate carboxykinase (Pck), and 3.8-fold ($p = 0.002$) aconitate hydratase 2.

An alternative to the glyoxylate shunt for acetate into glycolysis is the conversion of phosphoenol pyruvate (PEP) to pyruvate through pyruvate kinase (Pyk). From the glycolytic pathway, enzymes α-dehydro-β-deoxy-D-glucarate aldolase (GarL), Phosphoenol pyruvate synthetase (Pps) and enolase (Eno) showed a significant-fold increase when cells were grown on acetate (0.65; $p = 0.01$, 0.84; $p = 0.01$ and 2.77; $p < 10^{-6}$). Indeed, we observed higher phosphorylation fold for Pyk when cells were grown on glucose (2.8 fold increase; $p < 10^{-4}$). These results highlight that phosphorylated GarL, Pps and Eno may be significantly involved alongside Icd in regulating acetate metabolism.

< FIG. 3>

The ratios of phosphorylation for other glycolytic enzymes and sugar transporters also displayed significant changes. Protein phosphorylation is known to be important in transport of carbohydrate. Enzyme phosphoglycerate kinase (Pgk) was lower in acetate compared to glucose (2.35, $p = 0.006$). Enzyme Crr (PTS Enzyme IIA domain) showed a higher phosphorylation ratio (7.3-fold, $p < 10^{-6}$) on glucose. Enzymes involved in galactitol metabolism also displayed higher levels of phosphorylation on acetate, with phosphorylation events occurring in galactitol-specific enzyme IIA component of PTS (Gat A), galactitol-specific enzyme IIB component of PTS (Gat B), D-tagatose 1,6-bisphosphate aldolase 2, catalytic subunit (Gat Y) and D-tagatose 1,6-bisphosphate aldolase 2, subunit (Gat Z). While it is unclear the role of changes in phosphorylation ratio for enzymes involved in galactitol transport on acetate, the dynamics of the phosphorylation may suggest a pivotal role of phosphorylation in controlling transport. Changes in phosphorylation are probably linked to induction of carbon catabolic repression induction linked to acetate metabolism, yet the clear mechanism of co-regulation remains elusive. Finally, no significant changes were observed for fused mannose-specific PTS enzymes (ManX) or transaldolase B (talB) (Supplementary Fig. S2-7).

*3.4 Previously reported S/T/Y phosphorylations were found to be phosphorylated in H*

While designing our sMRM, we found several phosphorylations to occur in H rather than in S/T/Y, as reported previously. We found that most software that matches tandem mass spectra data with phosphorylated peptide sequences are biased towards S/T/Y phosphorylation. After trying different software to annotate phosphorylation sites and seeking expert advice from

Applied BioSciences (ABSciex), we found that phosphorylations in H are ignored. This reflects the fact that the majority of protein search engines were developed for eukaryotes. In eukaryotes, phosphorylation generally occurs in S/T/Y, and H phosphorylation is very rare compared to bacteria. Bacteria possess two-component systems which autophosphorylate H of the sensory kinase and D phosphorylation of the response regulator. This result in the specific signal recognition by the sensory kinase by activating its kinase activity, resulting in transfer of phosphor group to the response regulator, which triggers the cellular response, most often by binding to DNA sequences regulating gene transcription.

The paragon algorithm from ABSciex assigns weighted scores to phosphorylation sites: 0.35 to S/T/Y and only 0.01 to H. This result in miss-annotated protein phosphorylation sites, so the H score was changed 0.01 to 0.35 by changing the defaulting setting. Moreover, in an effort to validate all previously reported S/T/Y phosphorylation sites in *E. coli,* we undertook a careful evaluation of all phosphorylation sites in the Triple-TOF. First, the precursor mass of each reported phosphorylation ion was fixed. Second, the MS/MS for all fragment ions of the known mass was obtained. We named this approach ‘open scan IDA’. Finally, sMRM for unique m/z fragments were designed to validate phosphorylation sites.

Protein annotation software such as Protein Pilot and X! Tandem were unable to search MS/MS data from open scan IDA. Further expert advice from ABSciex suggested that search engine programs require a full MS scan to be able to parse all datasets. Therefore, a ‘dummy’ TOF scan was added to the Protein Pilot search file. This strategy also proved unsuccessful and none of Mascot, Protein Pilot or X! Tandem was able to search the open scan IDA files. Thus, a manual evaluation of tandem MS data was the only viable alternative (Fig. 4).

However, the number of phosphorylation possibilities in each peptide showed that manual evaluation was unfeasible for a large number of peptides for three reasons. First, manual evaluation of spectral data with more than three phosphorylation possibilities requires computational algorithms for analysis (Supplementary Table S3a). For example, finding unique ions for the phosphorylated elongation factor Tu (TufA) would mean manually searching for 448 possible masses. Second, some of the unique distinct masses that dictate the phosphorylation site are too small to be detected using standard MS instruments. For example, the two unique fragments for phosphorylated predicted protein (YdcY) and GMP synthetise (GuaA) were less than 200 Daltons (88 and 168 Da); standard proteomics MS parameters are typically set to detect masses larger than 200 Daltons (Supplementary Table S3b). Third, several unique masses were found to be shared among multiple phosphorylation possibilities. For example, the peptide HRDLLGATNPANALAGTR of multifunctional nucleoside diphosphate kinase (Ndk) enzyme shares masses 630.39 (±0.4), 635.35 (±0.01) and 489.19 (±0.5) among peptides charged +1 and +2 in different modification sites. Charge 635.3 corresponds to fragment b5 of the peptide charged +1 phosphorylated in both T and to fragment y13 of the peptide charged +2 phosphorylated in H (Supplementary Table S3c). Nonetheless, most of the parameters in IDA include more than two charges and are thus unable to correctly assign a phosphorylation site to the peptide.

Manual evaluation of phosphorylation site analysis resulted in the re-annotation of four proteins to H. Enzymes Ndk, GarL, polynucleotide phosphorylase/polyadenylase (Pnp) and inorganic pyrophosphatase (Ppa) (Supplementary Table S4a–b) were all found to be phosphorylated in H.

To validate the H phosphorylation, unique fragments had to be found by sMRM (Supplementary Fig. S8). Further, manual evaluation of spectral data confirmed S/T/Y phosphorylation for eight enzymes: Pps, protein chain elongation factor EF-Ts (Tsf), GatZ, predicted protein (YdcY), chaperone Hsp70 (DnaK), 50S ribosomal subunit protein L7/L12 (RplL) and predicted inner membrane protein (YbbP) (Supplementary Table S4c). This thorough evaluation also found S/T/Y miss-annotations. Enzyme GatZ was found to be phosphorylated in the T and the Y as opposed to the S and the T, as previously reported [15].

< FIG. 4>

## 4. Discussion

Protein phosphorylation is a common and well-studied post-translational modification. Evidence has accumulated confirming that S/T/Y phosphorylation is highly present in bacteria and has important regulatory roles [26-39, 41, 61]. Pioneering work by Macek and co-workers opened new avenues to identify hundreds of phosphorylation events in bacteria [14-16]. These studies led to important breakthroughs in the field of bacterial signalling, such as cross-talk between a S/T/Y kinase and a two-component H/D kinase found to be activated by YbdM-dependent phosphorylation [62]. In the last few years, evidence has accumulated to suggest that phosphorylation is a major mechanism of control of the central carbon metabolism of bacteria [12].

In our study, detection of phosphorylated peptides using ESI-MS/MS in IDA mode proved challenging in *E. coli*. Others have suggested that the poor ionisation capability of ESI, caused

by the negative charge suppression of phosphate groups, makes detection of phosphopeptides by ESI challenging [51]. Here we often found the proteins previously reported to be phosphorylated but the specific phosphorylated peptide was rarely detected. Therefore, to quantify global phosphorylation changes, sMRM [63-65]—which have been used successfully to detect and quantify low abundant metabolites and peptides in yeast [66] and in *S. erythraea* [40]—was used. As opposed to the use of the QSTAR, the QTRAP in sMRM mode was able to detect and quantify most phosphorylation peptides. Owing to the high sensitivity of sMRM, we performed a targeted label-free quantitation under changing culturing conditions. Label-free comparison of phosphorylation ratios (between phosphorylated and unphosphorylated cognates) proved reliable and reproducible across technical and biological replicates [40]. Notably, unlike isotopic quantification, samples were exempted from any additional manipulation. Further, sMRM offered the sensitivity that allowed us to precisely quantitate phosphorylation events. As such this work is a step forward in quantitatively understanding global and dynamic phosphorylation events in *E.coli*.

Significant changes in phosphorylation ratios were found for enzymes of the central carbon metabolism. Consistent with common knowledge, reversible phosphorylation of Icd showed that Icd regulates the partition of fluxes into the TCA cycle. This mechanism was the first example of phosphorylation control reported in a prokaryote [67]. Here we show that the glyoxylate shunt is in addition to other mechanisms of control [68], controlled by a cascade mechanism of post-translational modification [69] where, in addition to Icd, the ratio of phosphorylation for enzymes Mdh, Pck and AcnB change when cells are grown on acetate. Our data suggests that unphosphorylation of Mdh, Pck and AcnB plays a key role in activating and controlling the glyoxylate shunt. These observations are supported by other work that has observed post-

translational acetylation in regulation of acetate metabolism in *E. coli* BL21 [70]. Acetylation is controlled by the acetyltransferase, PatZ and deacetyltransferase cobB. The enzyme PatZ directly acetylates isocitrate lyase (AceA) and maybe isocitrate dehydrogenase phosphatase (AceK). The expression of *patZ* is regulated by catabolite repression, while *cobB* is constitutively expressed [71]. Findings of changing phosphorylation patterns in Mdh, Pck and AcnB contribute to demonstrate the tight mechanism of regulation by post-translational modification in the *E. coli* central carbon metabolism.

In line with this observation, a recent study where absolute quantification of the proteome with absolute determination of mRNA levels combined to flux analysis by statistical covariance analysis on A-stat experiments, showed that the central carbon metabolism of *E. coli* is predominantly controlled at the post-translational level [72]. To support this observation our data found several enzymes forming the central carbon metabolism of E. coli to have a dynamic phosphorylation profile under changing culture conditions, including Pyk, GarL, Pps, Eno, Pgk and Crr.

In Soares *et al.* (2013), it was shown that phosphorylation of stress-related proteins plays a role in controlling the early stages of growth. In accordance with these findings, this study demonstrates that chaperone DnaK displays a unique phosphorylation pattern. DnaK is a homolog of the eukaryotic Hsp70 chaperone system [73]. This chaperone system assists in a number of cytoplasmic cellular processes, including the folding of nascent polypeptide chains, the rescue of misfolded proteins, polypeptide chain translocation through membranes, and the assembly and disassembly of protein complexes. In a parallel investigation, a mutation in a Y

phosphatase-encoding gene led to decreased activity of these heat shock regulons [74]. Our data shows that when *E. coli* cells are under stress caused by acetate as the sole carbon source, a dramatic increase in phosphorylation is observed. This example confirms that by targeting key developmental enzymes, S/T/Y phosphorylation is able to control global changes in cellular metabolism.

We also show that annotation of phosphorylation sites is extremely challenging. For example, a recent publication (from the same authors) could detect only nine phosphorylated peptides that were previously phosphopeptides after $TiO_2$ enrichment and SCX fractionation [11]. While the authors were able to find nine phosphorylations in 30 enzymes previously reported, none of the peptides detected corresponded to those in the previous investigation. These results not only highlight the challenges involved in detecting phosphorylation events in bacteria but also point to several deficiencies in the field of bacterial phosphoproteomic. Of notable attention is the poor performance of software that assigns phosphorylations based on eukaryotic predictions and observations (and ignores H phosphorylation).

A large number of fragment ions are shared between different sites of phosphorylation within the same peptide; thus, assigning phosphorylation sites should require external validation such as sMRM design for unique fragment ions. To accurately detect phosphorylation sites in bacteria, it is imperative to set parameters carefully in the mass spectrometer and the protein discovery software in order to assign the correct phosphorylation sites. A careful analysis of MS/MS data from targeted open scan, suggests that GarL, Ndk, Pnp and Ppa previously annotated to be phosphorylated in S/T/Y are likely to be phosphorylated in H. These four enzymes were part of

the evolutionary conserved phosphorylation enzymes that built the evolutionary conserved theory reported in Macek *et al*. [15]. However, these phosphorylations are the active site of the enzyme. The use of synthetic peptides to disambiguate the assignment of complex PTMs, identical RT and MS/MS fragmentation patterns (which is beyond the scope of this investigation) can help elucidating and clarifying correct phosphorylation sites.

As mentioned in the introduction, the past-decade delivered many phosphoproteomics studies in phylogenetically diverse bacteria. Overall most of these studies reported numerous S/T/Y phosphorylation events, including isolated proteins where the role of phosphorylation has been elucidated and reviewed in detail elsewhere [58]. Yet, there is surprisingly little consistency in protein phosphorylation, even within closely related bacteria or within the same strains across studies (e.g. *E.coli* and *A. baumannii*) [15, 39]. Whether discrepancies reflect distinct biological role or technical variability due to MS discrepancies is unclear. In reality, to fully understand the physiological role of individual protein phosphorylation, *in vitro* and/or *in vivo* studies are needed. This has been done in engineered strains of *B. subtilis* [75] and *M. tuberculosis* [76]. Until such new strains are created, speculating on the specific or global role of S/T/Y phosphorylation in bacteria from global dynamic studies such as this study is challenging [12, 39, 40].

Nonetheless, it is evident that protein post-transcriptional modifications play an essential role in central metabolism control. This was recently shown in *E. coli* by integrating fluxes into absolute quantification of protein and transcripts [69]. By determining the regulation levels of metabolic fluxes for *E.coli* to achieve faster growth, it was found that post transcriptional modifications is the key mechanism of control of the *E. coli* central metabolism. Evidence is accumulating that

not only phosphorylation but other post-transcriptional modification are the key mechanisms of central metabolism control such as lysine acetylation [70].

## 5. Conclusion

The data presented here suggest that, as in eukaryotes, global phosphorylation changes mediate bacterial metabolism. Protein phosphorylation participates in many critical cellular processes and provides the basis for a detailed high-resolution, functional quantitative analysis of post-translational modification in bacteria. The data from this investigation and the sMRM workflow provide a useful example of a data-driven targeted phosphoproteomic approach in which several new mechanisms of control are linked to unique metabolic behaviours. We confirmed that sMRM is suitable for detecting extremely rare phosphorylation events and for quantitating these phosphorylations under changing culture conditions. Further, the data demonstrate that changes in the phosphorylation ratio in enzymes from the *E. coli* central carbon metabolism are controlled by S/T/Y phosphorylation.



## Acknowledgements

We gratefully acknowledge Alun Jones and Amanda Nouwens for his/her technical assistance with the LC-MS/MS and helpful insight over the entire course of this investigation. We thank the Proteomics facility at IMB and SCMB. We are thankful to Michael Wang for his help with the SCX separation, to Haryadi Sugiarto for assisting in operating the bioreactor and also to Robert

Speight and Colin Archer for reviewing the manuscript. This work was supported by funds from the Australian Government.

## Appendix A. Abbreviations

H/D – Histidine (H) and Aspartate (D)

IDA – Information-dependent acquisition

LB – Luria Bertani

LLD – Lowest limit of detection

MIDAS – Multiple reaction monitoring-initiated detection and sequencing

sMRM - Scheduled multiple reaction monitoring

S/T/Y – Serine (S) Threonine (T) and Tyrosine (Y)

SCX – Strong cation exchange

## Appendix B. Supplementary data

**References**

[1] Beltrao P, Bork P, Krogan NJ, van Noort V. Evolution and functional cross-talk of protein post-translational modifications. Mol Syst Biol. 2013;9:714.
[2] Stock JB, Ninfa AJ, Stock AM. Protein phosphorylation and regulation of adaptive responses in bacteria. Microbiol Rev. 1989;53:450-90.
[3] Parkinson JS, Kofoid EC. Communication modules in bacterial signaling proteins. Annu Rev Genet. 1992;26:71-112.
[4] Grangeasse C, Cozzone AJ, Deutscher J, Mijakovic I. Tyrosine phosphorylation: an emerging regulatory device of bacterial physiology. Trends Biochem Sci. 2007;32:86-94.
[5] Macek B, Mijakovic I. Site-specific analysis of bacterial phosphoproteomes. Proteomics. 2011;11:3002-11.
[6] Derouiche A, Cousin C, Mijakovic I. Protein phosphorylation from the perspective of systems biology. Curr Opin Biotechnol. 2012;23:585-90.
[7] Kyriakis JM. In the Beginning, There Was Protein Phosphorylation. Journal of Biological Chemistry. 2014:jbc. R114. 557926.
[8] Stock AM, Robinson VL, Goudreau PN. Two-component signal transduction. Annu Rev Biochem. 2000;69:183-215.
[9] Baker MD, Stock JB. Signal transduction: networks and integrated circuits in bacterial cognition. Curr Biol. 2007;17:R1021-4.
[10] Deutscher J, Saier MH, Jr. Ser/Thr/Tyr protein phosphorylation in bacteria - for long time neglected, now well established. J Mol Microbiol Biotechnol. 2005;9:125-31.
[11] Soufi B, Soares NC, Ravikumar V, Macek B. Proteomics reveals evidence of cross-talk between protein modifications in bacteria: focus on acetylation and phosphorylation. Curr Opin Microbiol. 2012;15:357-63.
[12] Soares NC, Spat P, Krug K, Macek B. Global dynamics of the Escherichia coli proteome and phosphoproteome during growth in minimal medium. J Proteome Res. 2013;12:2611-21.

[13] Jers C, Soufi B, Grangeasse C, Deutscher J, Mijakovic I. Phosphoproteomics in bacteria: towards a systemic understanding of bacterial phosphorylation networks. Expert Rev Proteomic. 2008;5:619-27.
[14] Macek B, Mijakovic I, Olsen JV, Gnad F, Kumar C, Jensen PR, et al. The serine/threonine/tyrosine phosphoproteome of the model bacterium Bacillus subtilis. Mol Cell Proteomics. 2007;6:697-707.
[15] Macek B, Gnad F, Soufi B, Kumar C, Olsen JV, Mijakovic I, et al. Phosphoproteome Analysis of E. coli Reveals Evolutionary Conservation of Bacterial Ser/Thr/Tyr Phosphorylation. Mol Cell Proteomics. 2008;7:299-307.
[16] Soufi B, Gnad F, Jensen PR, Petranovic D, Mann M, Mijakovic I, et al. The Ser/Thr/Tyr phosphoproteome of Lactococcus lactis IL1403 reveals multiply phosphorylated proteins. Proteomics. 2008;8:3486-93.
[17] Manai M, Cozzone AJ. Analysis of the protein-kinase activity of Escherichia coli cells. Biochem Biophys Res Commun. 1979;91:819-26.
[18] Wang JY, Koshland DE, Jr. Evidence for protein kinase activities in the prokaryote Salmonella typhimurium. J Biol Chem. 1978;253:7605-8.
[19] van Dijk AA, de Lange LC, Bachovchin WW, Robillard GT. Effect of phosphorylation on hydrogen-bonding interactions of the active site histidine of the phosphocarrier protein HPr of the phosphoenolpyruvate-dependent phosphotransferase system determined by 15N NMR spectroscopy. Biochemistry. 1990;29:8164-71.
[20] Reizer J, Romano AH, Deutscher J. The role of phosphorylation of HPr, a phosphocarrier protein of the phosphotransferase system, in the regulation of carbon metabolism in gram-positive bacteria. J Cell Biochem. 1993;51:19-24.
[21] Mijakovic I, Poncet S, Galinier A, Monedero V, Fieulaine S, Janin J, et al. Pyrophosphate-producing protein dephosphorylation by HPr kinase/phosphorylase: a relic of early life? Proc Natl Acad Sci U S A. 2002;99:13442-7.
[22] Zhang P, Ma Y, Wang F, Wei D. Phosphorylation of HPr by HPr Kinase in Gluconobacter oxydans 621H. Protein Pept Lett. 2014.

[23] Stueland CS, Gorden K, LaPorte DC. The isocitrate dehydrogenase phosphorylation cycle. Identification of the primary rate-limiting step. J Biol Chem. 1988;263:19475-9.
[24] Laporte DC, Stueland CS, Ikeda TP. Isocitrate dehydrogenase kinase/phosphatase. Biochimie. 1989;71:1051-7.
[25] LaPorte DC. The isocitrate dehydrogenase phosphorylation cycle: regulation and enzymology. J Cell Biochem. 1993;51:14-8.
[26] Lin MH, Hsu TL, Lin SY, Pan YJ, Jan JT, Wang JT, et al. Phosphoproteomics of Klebsiella pneumoniae NTUH-K2044 reveals a tight link between tyrosine phosphorylation and virulence. Mol Cell Proteomics. 2009;8:2613-23.
[27] Ravichandran A, Sugiyama N, Tomita M, Swarup S, Ishihama Y. Ser/Thr/Tyr phosphoproteome analysis of pathogenic and non-pathogenic Pseudomonas species. Proteomics. 2009;9:2764-75.
[28] Parker JL. Analysis of the phosphoproteome of the multicellular bacterium Streptomyces coelicolor A3(2) by protein/peptide fractionation, phosphopeptide enrichment and high-accuracy mass spectrometry (vol 10, pg 2486, 2010). Proteomics. 2010;10:3056-.
[29] Manteca A, Ye J, Sanchez J, Jensen ON. Phosphoproteome analysis of Streptomyces development reveals extensive protein phosphorylation accompanying bacterial differentiation. J Proteome Res. 2011;10:5481-92.
[30] Sun X, Ge F, Xiao CL, Yin XF, Ge R, Zhang LH, et al. Phosphoproteomic analysis reveals the multiple roles of phosphorylation in pathogenic bacterium Streptococcus pneumoniae. J Proteome Res. 2010;9:275-82.
[31] Schmidl SR, Gronau K, Pietack N, Hecker M, Becher D, Stulke J. The phosphoproteome of the minimal bacterium Mycoplasma pneumoniae: analysis of the complete known Ser/Thr kinome suggests the existence of novel kinases. Mol Cell Proteomics. 2010;9:1228-42.
[32] Misra SK, Milohanic E, Ake F, Mijakovic I, Deutscher J, Monnet V, et al. Analysis of the serine/threonine/tyrosine phosphoproteome of the pathogenic bacterium

Listeria monocytogenes reveals phosphorylated proteins related to virulence. Proteomics. 2011;11:4155-65.
[33] Ge R, Sun X, Xiao C, Yin X, Shan W, Chen Z, et al. Phosphoproteome analysis of the pathogenic bacterium Helicobacter pylori reveals over-representation of tyrosine phosphorylation and multiply phosphorylated proteins. Proteomics. 2011;11:1449-61.
[34] Bai X, Ji Z. Phosphoproteomic investigation of a solvent producing bacterium Clostridium acetobutylicum. Appl Microbiol Biotechnol. 2012;95:201-11.
[35] Hu CW, Lin MH, Huang HC, Ku WC, Yi TH, Tsai CF, et al. Phosphoproteomic analysis of Rhodopseudomonas palustris reveals the role of pyruvate phosphate dikinase phosphorylation in lipid production. J Proteome Res. 2012;11:5362-75.
[36] Takahata Y, Inoue M, Kim K, Iio Y, Miyamoto M, Masui R, et al. Close proximity of phosphorylation sites to ligand in the phosphoproteome of the extreme thermophile Thermus thermophilus HB8. Proteomics. 2012;12:1414-30.
[37] Yang MK, Qiao ZX, Zhang WY, Xiong Q, Zhang J, Li T, et al. Global phosphoproteomic analysis reveals diverse functions of serine/threonine/tyrosine phosphorylation in the model cyanobacterium Synechococcus sp. strain PCC 7002. J Proteome Res. 2013;12:1909-23.
[38] Basell K, Otto A, Junker S, Zuhlke D, Rappen GM, Schmidt S, et al. The phosphoproteome and its physiological dynamics in Staphylococcus aureus. Int J Med Microbiol. 2014;304:121-32.
[39] Soares NC, Spat P, Mendez JA, Nakedi K, Aranda J, Bou G. Ser/Thr/Tyr phosphoproteome characterization of Acinetobacter baumannii: Comparison between a reference strain and a highly invasive multidrug-resistant clinical isolate. J Proteomics. 2014.
[40] Licona-Cassani C, Lim S, Marcellin E, Nielsen LK. Temporal dynamics of the Saccharopolyspora erythraea phosphoproteome. Mol Cell Proteomics. 2014;13:1219-30.
[41] Prisic S, Dankwa S, Schwartz D, Chou MF, Locasale JW, Kang CM, et al. Extensive phosphorylation with overlapping specificity by Mycobacterium tuberculosis serine/threonine protein kinases. Proc Natl Acad Sci U S A. 2010;107:7521-6.

[42] Elsholz AK, Turgay K, Michalik S, Hessling B, Gronau K, Oertel D, et al. Global impact of protein arginine phosphorylation on the physiology of Bacillus subtilis. Proc Natl Acad Sci U S A. 2012;109:7451-6.
[43] Mijakovic I, Macek B. Impact of phosphoproteomics on studies of bacterial physiology. FEMS Microbiol Rev. 2012;36:877-92.
[44] Koponen J, Laakso K, Koskenniemi K, Kankainen M, Savijoki K, Nyman TA, et al. Effect of acid stress on protein expression and phosphorylation in Lactobacillus rhamnosus GG. J Proteomics. 2012;75:1357-74.
[45] Schmidt A, Trentini DB, Spiess S, Fuhrmann J, Ammerer G, Mechtler K, et al. Quantitative phosphoproteomics reveals the role of protein arginine phosphorylation in the bacterial stress response. Mol Cell Proteomics. 2014;13:537-50.
[46] Cozzone AJ. Role of protein phosphorylation on serine/threonine and tyrosine in the virulence of bacterial pathogens. J Mol Microbiol Biotechnol. 2005;9:198-213.
[47] Whitmore SE, Lamont RJ. Tyrosine phosphorylation and bacterial virulence. Int J Oral Sci. 2012;4:1-6.
[48] Boulanger A, Chen Q, Hinton DM, Stibitz S. In vivo phosphorylation dynamics of the Bordetella pertussis virulence-controlling response regulator BvgA. Mol Microbiol. 2013;88:156-72.
[49] Hansen AM, Chaerkady R, Sharma J, Diaz-Mejia JJ, Tyagi N, Renuse S, et al. The Escherichia coli phosphotyrosine proteome relates to core pathways and virulence. PLoS Pathog. 2013;9:e1003403.
[50] Martinez MA, Das K, Saikolappan S, Materon LA, Dhandayuthapani S. A serine/threonine phosphatase encoded by MG_207 of Mycoplasma genitalium is critical for its virulence. BMC Microbiol. 2013;13:44.
[51] Gropengiesser J, Varadarajan BT, Stephanowitz H, Krause E. The relative influence of phosphorylation and methylation on responsiveness of peptides to MALDI and ESI mass spectrometry. J Mass Spectrom. 2009;44:821-31.
[52] Nakamura T, Myint KT, Oda Y. Ethylenediaminetetraacetic acid increases identification rate of phosphoproteomics in real biological samples. J Proteome Res. 2010;9:1385-91.

[53] Shilov IV, Seymour SL, Patel AA, Loboda A, Tang WH, Keating SP, et al. The Paragon Algorithm, a next generation search engine that uses sequence temperature values and feature probabilities to identify peptides from tandem mass spectra. Mol Cell Proteomics. 2007;6:1638-55.
[54] Cox DM, Zhong F, Du M, Duchoslav E, Sakuma T, McDermott JC. Multiple reaction monitoring as a method for identifying protein posttranslational modifications. J Biomol Tech. 2005;16:83-90.
[55] Unwin RD, Griffiths JR, Leverentz MK, Grallert A, Hagan IM, Whetton AD. Multiple reaction monitoring to identify sites of protein phosphorylation with high sensitivity. Mol Cell Proteomics. 2005;4:1134-44.
[56] Song E, Pyreddy S, Mechref Y. Quantification of glycopeptides by multiple reaction monitoring liquid chromatography/tandem mass spectrometry. Rapid Commun Mass Spectrom. 2012;26:1941-54.
[57] Grote E, Fu Q, Ji W, Liu X, Van Eyk JE. Using pure protein to build a multiple reaction monitoring mass spectrometry assay for targeted detection and quantitation. Methods Mol Biol. 2013;1005:199-213.
[58] Dworkin J. Ser/Thr phosphorylation as a regulatory mechanism in bacteria. Current Opinion in Microbiology. 2015;24:47-52.
[59] Pereira SF, Goss L, Dworkin J. Eukaryote-like serine/threonine kinases and phosphatases in bacteria. Microbiol Mol Biol Rev. 2011;75:192-212.
[60] Shenolikar S. Protein serine/threonine phosphatases--new avenues for cell regulation. Annual review of cell biology. 1994;10:55-86.
[61] Licona-Cassani C, Lim S, Marcellin E, Nielsen LK. Temporal dynamics of the Saccharopolyspora erythraea phosphoproteome. Mol Cell Proteomics. 2014.
[62] Jers C, Kobir A, Sondergaard EO, Jensen PR, Mijakovic I. Bacillus subtilis Two-Component System Sensory Kinase DegS Is Regulated by Serine Phosphorylation in Its Input Domain. PLoS One. 2011;6.
[63] Unwin RD, Griffiths JR, Whetton AD. A sensitive mass spectrometric method for hypothesis-driven detection of peptide post-translational modifications: multiple

reaction monitoring-initiated detection and sequencing (MIDAS). Nat Protoc. 2009;4:870-7.
[64] Yocum AK, Chinnaiyan AM. Current affairs in quantitative targeted proteomics: multiple reaction monitoring-mass spectrometry. Brief Funct Genomic Proteomic. 2009;8:145-57.
[65] Wolf-Yadlin A, Hautaniemi S, Lauffenburger DA, White FM. Multiple reaction monitoring for robust quantitative proteomic analysis of cellular signaling networks. Proc Natl Acad Sci U S A. 2007;104:5860-5.
[66] Oliveira AP, Ludwig C, Picotti P, Kogadeeva M, Aebersold R, Sauer U. Regulation of yeast central metabolism by enzyme phosphorylation. Mol Syst Biol. 2012;8:623.
[67] Cozzone AJ. Regulation of acetate metabolism by protein phosphorylation in enteric bacteria. Annu Rev Microbiol. 1998;52:127-64.
[68] Valgepea K, Adamberg K, Nahku R, Lahtvee P-J, Arike L, Vilu R. Systems biology approach reveals that overflow metabolism of acetate in Escherichia coli is triggered by carbon catabolite repression of acetyl-CoA synthetase. BMC Systems Biology. 2010;4:166.
[69] Arifin Y, Archer C, Lim S, Quek L-E, Sugiarto H, Marcellin E, et al. Escherichia coli W shows fast, highly oxidative sucrose metabolism and low acetate formation. Appl Microbiol Biot. 2014;98:9033-44.
[70] Castano-Cerezo S, Bernal V, Rohrig T, Termeer S, Canovas M. Regulation of acetate metabolism in Escherichia coli BL21 by protein N-epsilon-lysine acetylation. Appl Microbiol Biot. 2015;99:3533-45.
[71] Castano-Cerezo S, Bernal V, Blanco-Catala J, Iborra JL, Canovas M. cAMP-CRP co-ordinates the expression of the protein acetylation pathway with central metabolism in Escherichia coli. Mol Microbiol. 2011;82:1110-28.
[72] Valgepea K, Adamberg K, Seiman A, Vilu R. Escherichia coli achieves faster growth by increasing catalytic and translation rates of proteins. Mol Biosyst. 2013;9:2344-58.
[73] Bukau B, Horwich AL. The Hsp70 and Hsp60 chaperone machines. Cell. 1998;92:351-66.

[74] Klein G, Dartigalongue C, Raina S. Phosphorylation-mediated regulation of heat shock response in Escherichia coli. Mol Microbiol. 2003;48:269-85.
[75] Ravikumar V, Shi L, Krug K, Derouiche A, Jers C, Cousin C, et al. Quantitative phosphoproteome analysis of Bacillus subtilis reveals novel substrates of the kinase PrkC and phosphatase PrpC. Mol Cell Proteomics. 2014;13:1965-78.
[76] Parandhaman DK, Sharma P, Bisht D, Narayanan S. Proteome and phosphoproteome analysis of the serine/threonine protein kinase E mutant of Mycobacterium tuberculosis. Life Sci. 2014;109:116-26.

**Figure captions**

**Fig. 1** Purified α-casein in its phosphorylated and unphosphorylated form was purchased from Sigma to test whether phosphopeptides are inherently difficult to discover by LC-MS/MS. Also, α-casein was used to validate our sMRM approach. (A) shows the lowest limit of detection (LLD) for 4 phosphopeptides of α-casein. After spiking an *E. coli* protein digest with α-casein (a 'complex matrix'), we found that the complex background increased the limit of detection of each individual peptide, while phosphopeptides and peptides had a similar LLD. (B) displays the ratios of phosphorylated and unphosphorylated peptides. A consistent decrease in intensity for phosphorylated peptides was observed. (C) show sMRM for YKVPQLEIVPNSAEER 3+/y7 peptide from α-casein. The Fig. represents the percentage ratio of phosphorylations versus unphosphorylated peptides (nP: unphosphorylated, P: phosphorylated).

**Fig. 2** Phosphorylations in central carbon metabolisms (glycolysis, TCA and PPP). The metabolic pathway shows the phosphorylation ratio under three different carbon sources. Samples are ordered by phosphorylation ratios, where G, A and LB represent R/2 plus glucose (G), M9 plus acetate (A) and LB.

**Fig. 3** Validation and quantitative measurements for Icd cultured under glucose and acetate. (A) shows the spectrum for discovery mode for peptide SLNVALR. As observed, the overall intensity of all fragmented ions is higher on acetate versus glucose. In (B) and (C), each chromatogram represents the peak area from cells grown on glucose and acetate. (B) is a chromatogram of sMRM for SLNVALR +2/y4 before TiO2 enrichment. (C) is a chromatogram

of sMRM for SLNVALR +2/y4 after TiO2 enrichment (nP: unphosphorylation, P: phosphorylation).

**Fig. 4** Chromatograms for IDA and sMRM for GarL. The chromatograms were manually examined to establish the correct phosphorylation site. Even a small peptide containing only 7 amino acids has three phosphorylation possibilities. Out of 14 possible fragment ions, 8 ions (shown in light orange in Fig. 4A) are shared between all three phosphorylation possibilities. Mass ions (shown in grey or light purple) are shared between at least two phosphorylation possibilities. Only 4 ions (shown in yellow) and 2 ions (shown in light green) are unique for the first S and H modification (Fig. 4A). Although this peptide had been reported to be modified in S [15], detailed analysis of the open scan MS/MS showed that phosphorylation occurs in the H and not in the S (Fig. 4B, and masses coloured red in Fig. 4A). (C) Unique b5 and y4 ions found to be phosphorylated in H by sMRM analysis (b5; 430.23, y4; 576.23).

**Fig. 1**

A **Lower limit of detection**

| Peptides | Modification site | Complex matrix ($\mu g^{*}\mu L^{-1}$) P | Complex matrix nP | Distilled water P | Distilled water nP |
|---|---|---|---|---|---|
| DIGSESTEDQAMEDIK | PhoIS) @4; Pho(S)@6 | 0.87 | 0.87 | 0.08 | <0.05 |
| YKVPQLEIVPNSAEER | Pho(S) @12 | 0.87 | 0.87 | 0.02 | 0.02 |
| TVDMESTEVFTKK | Pho(S) @6 | 1.07 | 1.07 | 0.08 | 0.04 |
| VPQLEIVPNSAEER | Pho(S) @10 | 1.29 | 1.29 | 0.08 | 0.08 |

B

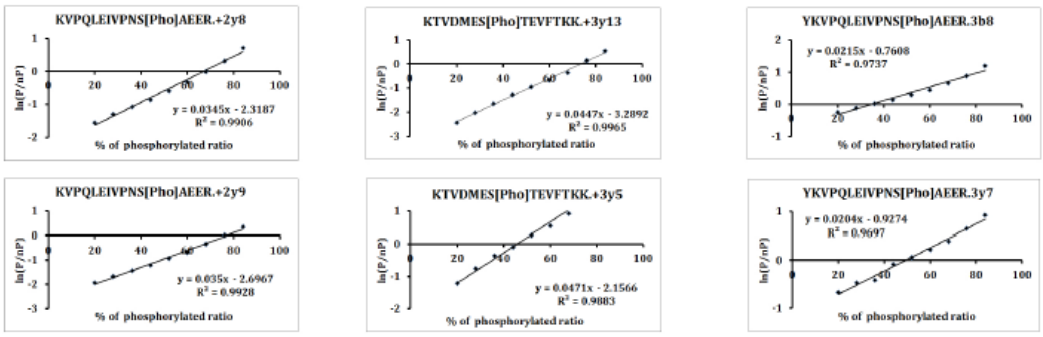


C

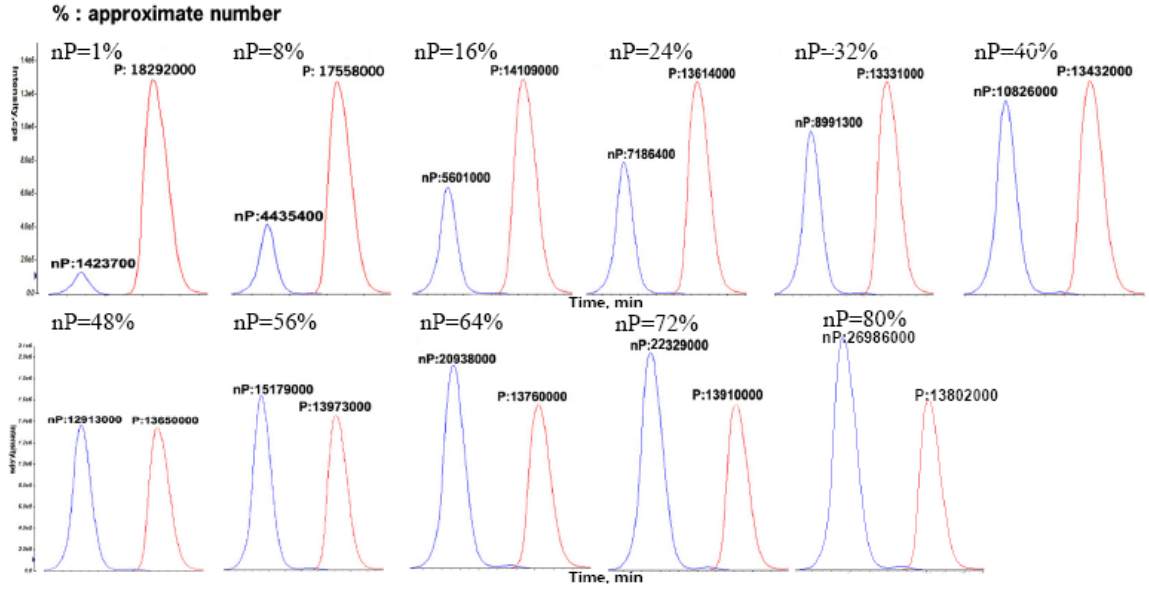

**Fig. 2**

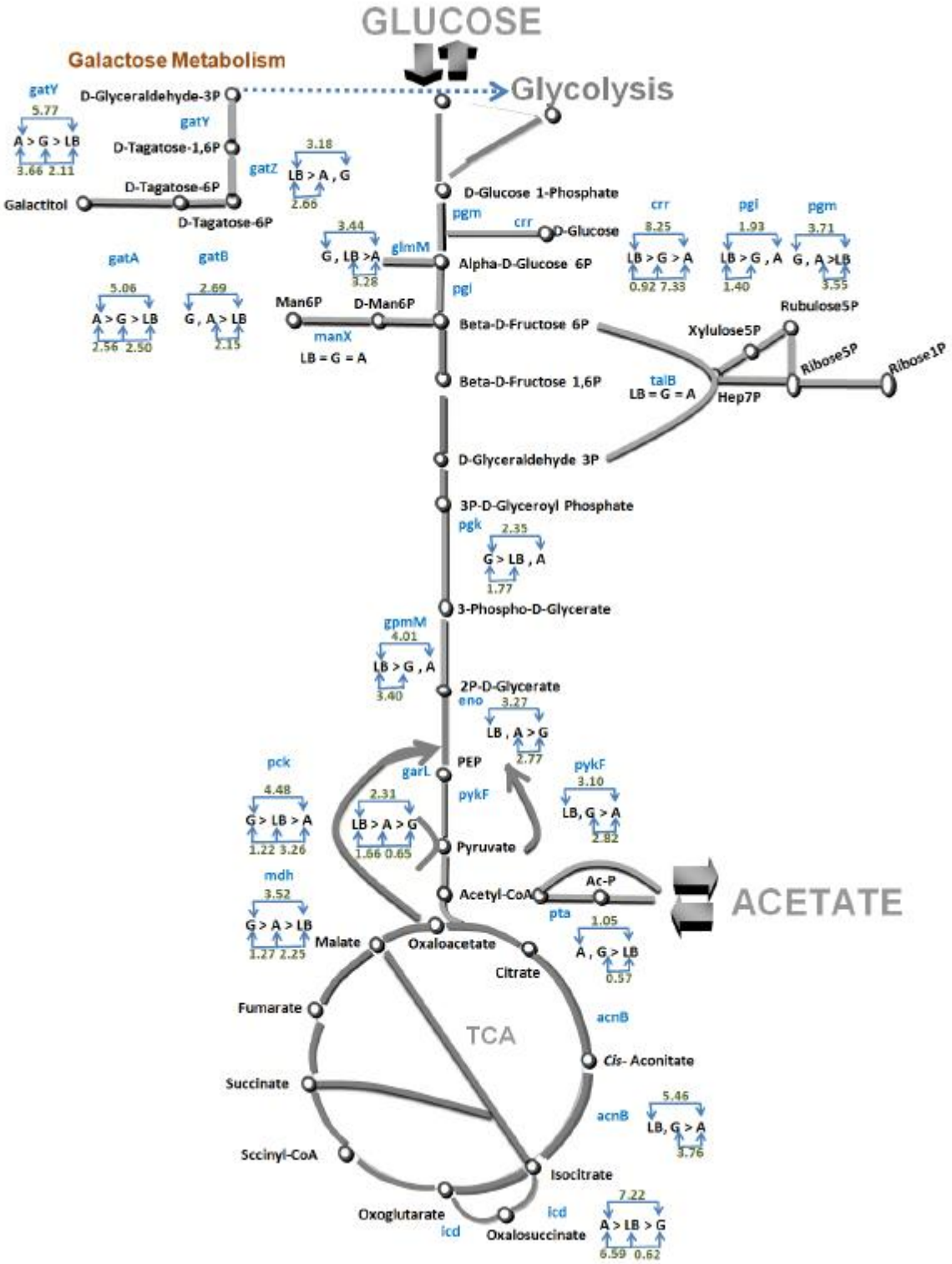

**Fig. 3**

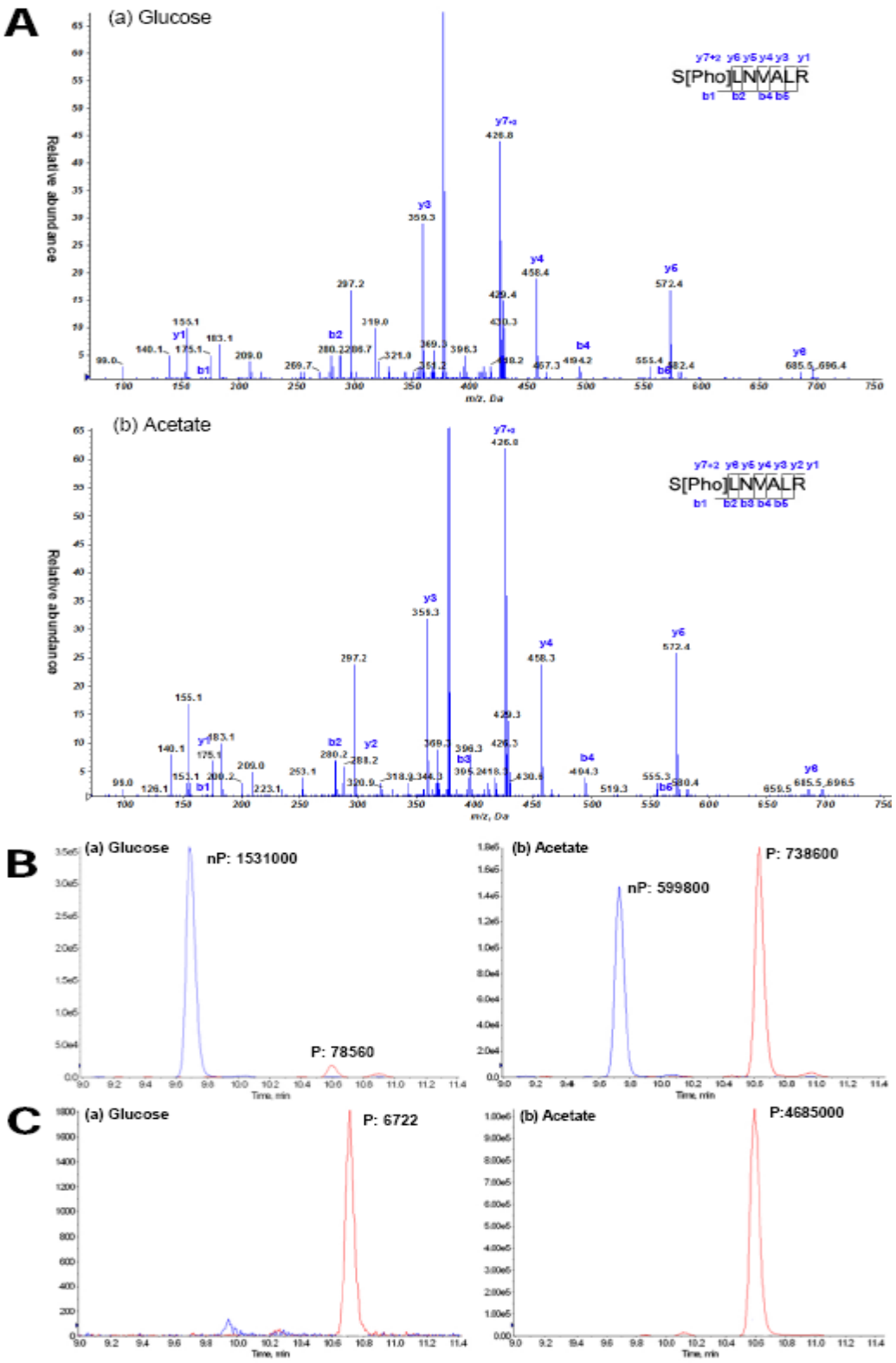

**Fig. 4**

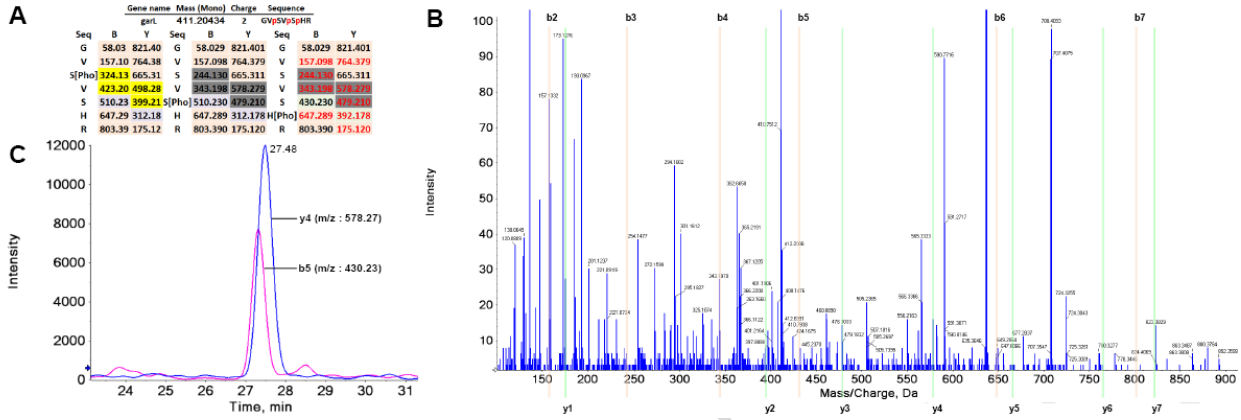

**Graphical abstract**

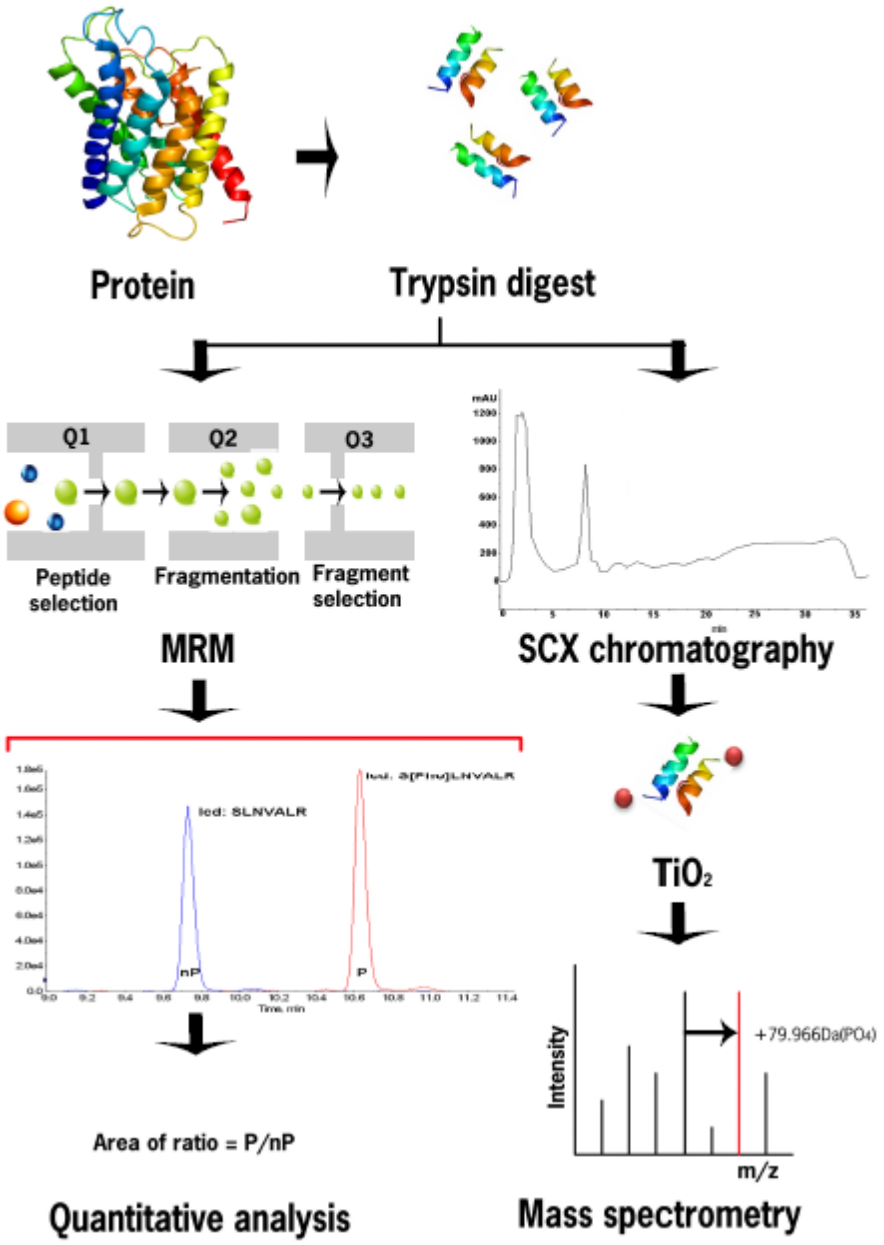

Highlights

- Validation of sMRM approach to quantify ratios of phosphorylation
- Phosphorylation ratios changed under changing culture conditions (carbone source: acetate, glucose or LB medium)
- The ratio of phosphorylation for 23 enzymes from central carbon metabolism was found to be dynamic.
- Manual evaluation of phosphorylation sites